Catalysis Science & Technology

Accepted Manuscript

This article can be cited before page numbers have been issued, to do this please use: R. Ferraccioli, D. Borovika, A. Surkus, C. R. Kreyenschulte, C. Topf and M. Beller, *Catal. Sci. Technol.*, 2017, DOI: 10.1039/C7CY01577A.

ROYAL SOCIETY OF CHEMISTRY

rsc.li/catalysis

View Article Online
DOI: 10.1039/C7CY01577A

Journal Name

ARTICLE

Synthesis of Cobalt Nanoparticles by Pyrolysis of Vitamin B_{12}: A Non-noble Catalyst for Efficient Hydrogenation of Nitriles

Received 00th January 20xx,
Accepted 00th January 20xx

DOI: 10.1039/x0xx00000x

www.rsc.org/

Raffaella Ferraccioli,[a,b] Diana Borovika,[a] Annette-Enrica Surkus,[a] Carsten Kreyenschulte,[a] Christoph Topf *[a,c] and Matthias Beller *[a]

A facile preparation of vitamin B_{12}-derived carbonaceous cobalt particles supported on ceria is reported. The resulting composite material is obtained upon wet impregnation of ceria with natural cyanocobalamin and consecutive pyrolysis under inert conditions. The novel catalyst shows good to excellent performance in the industrially relevant heterogeneous hydrogenation of nitriles to the corresponding primary amines.

1. Introduction

Heterogeneous catalysts incorporating heteroatom doped graphene entities adopt a vital role as functional materials in both synthesis[1] and energy[2] related contexts. Applying N, B, P and S as dopants allows to alter significantly the electronic and physicochemical properties of both the supported metal and the carrier material.[3] This enables the development of high performance materials with tailor-made properties. In the past decade, especially nitrogen doped graphenes (NGr's) combined with transition metals emerged as effective catalytic systems that govern a wide field of applications including reductions,[4] oxidations,[5] C-C bond formation,[6] oxygen reduction reactions (ORR),[7] hydrogen evolution reactions (HER),[8] and photocatalysis.[9]

During the course of the last four years, we reported on the synthesis and application of a variety of metal-based nanocomposites supported on Vulcan® XC 72 R carbon,[10,11] and α-alumina[12]. In general, these hybrid materials were obtained upon wet impregnation of the carrier material with a solution containing an *in situ* generated metal-phenanthroline chelate, followed by desiccation and pyrolysis of the initially adsorbed complex. Using cobalt-phenanthroline, the resulting heterogeneous materials feature a core shell architecture in which Co-based nanoparticles of different size are enveloped by *N*-doped graphene sheets.

In this context, the utilization of abundant and bio-available metalliferous (co)enzymes as impregnating agents represents an attractive alternative for the convenient preparation of novel carbon-augmented heterogeneous metal catalysts. By virtue of their inherent metal and high nitrogen content coenzyme B_{12} and in particular the molecular less complicated and much lower-priced congener vitamin B_{12}[13] (cyanocobalamin) are interesting starting materials for crafting supported Co-NGr type catalysts.

Notably, the deployment of vitamin B_{12} as solution phase precursor offers crucial advantages for the preparation of heterogenised metal complexes. Since cyanocobalamin represents a prefabricated cobalt macrocyclic complex, the extra chelation step of the catalytically active metal with added N-donor ligand prior to support impregnation is superfluous. Hence, the overall synthesis of the catalyst described herein is convenient and time-saving. In addition, the polar groups decorating the periphery of the corrin scaffold render vitamin B_{12} non-sublimable. Therefore, the pyrolysis procedure is not hampered by partial volatilization of initially adsorbed organic material.

Hitherto, only a few reports on thermally modified cyanocobalamin used as catalytically active material appeared in the literature. Applications have been reported for the oxygen reduction reaction[14] in fuel cells and as functional material for electrocatalytic hydrogen evolution.[15] Moreover, one catalytic protocol for oxidative imine synthesis mediated by mesoporous carbon obtained through pyrolysis of natural vitamin B_{12} appeared recently.[16]

Herein, we elaborate the catalytic potential of a thermally decomposed Co-corrin assembly by attaching cyanocobalamin onto ceria *via* wet impregnation and subsequent pyrolysis under inert conditions. We selected this support due to its excellent inherent thermal stability, beneficial acid-base behavior and peculiar redox surface properties.[17] The catalytic performance of the thus obtained materials is successfully demonstrated in the atom efficient and industrially relevant hydrogenation of nitriles to primary amines which adopts a pivotal role in the large-scale production of pharmaceuticals, dyes and agrochemicals.[18a] Amongst the known procedures for the synthesis of primary amines, reduction of nitriles constitutes a common approach. In the past nitriles have been

[a] Leibniz-Institut für Katalyse e.V. an der Universität Rostock, Albert-Einstein-Straße 29a, 18059 Rostock, Germany.
[b] CNR-Istituto di Scienze e Tecnologie Molecolari (ISTM), Via C. Golgi 19, 20133 Milano, Italy
[c] Institut für Katalyse-Johannes Kepler Universität Linz, Altenberger Straße 69, 4040 Linz, Austria.

View Article Online
DOI: 10.1039/C7CY01577A

often reduced using metal hydrides such as $LiAlH_4$ or $NaBH_4$. However, these methodologies have drawbacks in terms of selectivity and generation of waste. In contrast, direct hydrogenation of nitriles is greener and more sustainable.[18b-e] Notably, a similar approach to the here presented work for hydrogenation of aromatic nitriles was achieved using Pd/C.[18f]

2. Experimental

2.1. General

The general hydrogenation reactions were conducted in 8 mL glass vials which were placed in a 300 mL autoclave (PARR Instrument Company). Conversions and yields of the hydrogenation reactions were determined by a GC-FID device (HP 6890), capillary column HP-5 (30 m x 250 mm x 0.25 µm). Mass spectra were recorded on an Agilent 5973 GC-MS spectrograph. ^{1}H NMR spectra of the compounds were recorded on a 300 MHz (Bruker AV-300) or 400 MHz (Bruker AV-400) spectrometer; $^{13}C\{^1H\}$ NMR spectra were obtained at 75 MHz or 101 MHz, respectively. CHN analyses were performed using a Leco Microanalysator TruSpec. The metal content of the catalysts was determined by atom absorption spectroscopy using a PerkinElmer AAS Analyst 300 or by emissions spectroscopy (ICP) using a Varian 715-ES after fusion melts and acidic dissolving of the sample. XRD pattern of the materials were recorded on a PANalytical X'Pert Pro diffractometer in reflection mode with Cu Kα radiation (λ=1.5406 Å) and a silicon strip detector (X'Celerator). XPS data were obtained with a VG ESCALAB220iXL (ThermoScientific) with monochromatic Al Kα (1486.6 eV) radiation. The electron binding energies E_B were obtained without charge compensation. For quantitative analysis the peaks were deconvoluted with Gaussian-Lorentzian curves, the peak area was divided by a sensitive factor obtained from the element specific Scofield factor and the transmission function of the spectrometer. The TEM measurements were performed at 200kV with a probe aberration-corrected JEM-ARM200F (JEOL, Corrector: CEOS). The microscope is equipped with a JED-2300 (JEOL) energy-dispersive x-ray-spectrometer (EDXS) for chemical analysis. The aberration corrected STEM imaging (High-Angle Annular Dark Field (HAADF) and Annular Bright Field (ABF)) were performed under the following conditions. HAADF and ABF both were done with a spot size of approximately 0.13nm, a convergence angle of 32-36 mrad and collection semi-angles for HAADF and ABF of 90-170 mrad and 11-22 mrad respectively. Preparation of the TEM sample was deposed on a holey carbon supported Cu-grid (mesh 300) without any pretreatment and transferred to the microscope.

2.2. Catalyst preparation

A set of heterogeneous catalysts each obtained upon thermal heat treatment of vitamin B_{12}-impregnated ceria support (cyanocobalamine from Fisher BioReagents and cerium(IV)oxide nanopowder from Sigma-Aldrich) was prepared according to the previous synthesis of a related Co_3O_4/NGr@CeO_2 nanocomposite prepared from a cobalt-phenanthroline-chelate.[19] To a deep purple solution of cyanocobalamin (338.8 mg, 0.25 mmol, is equivalent to 15 mg of cobalt) in EtOH (50 mL) was added cerium(IV)oxide nanopowder (1.0 g) to obtain a material containing 1.5 wt% of Co/CeO_2. The mixture was heated at reflux under magnetic stirring for 4 h. After cooling to room temperature the solvent was evaporated under reduced pressure. The solid residue was dried under vacuum for 4 h at r.t. The dry solid was grinded to a fine powder, transferred into a ceramic crucible and placed in the oven. The oven was evacuated to 5 mbar and then flushed with argon. The furnace was then heated to 800 °C (or 700, 900 and 1000 °C, respectively) at a rate of 25 °C per minute and held at the required temperature for 2 h under an argon atmosphere. After that, heating was stopped and the oven was allowed to reach room temperature. During the whole process argon was constantly passed through the interior of the furnace. Hereinafter, the catalysts obtained upon pyrolysis at 700, 800, 900 and 1000 °C respectively, are referred to as B_{12}@CeO_2-X; X: 7, 8, 9 or 10.

2.3. General procedure for the hydrogenation of nitriles

A glass vial fitted with a magnetic stirring bar and a septum cap penetrated with a needle was charged with the B_{12}@CeO_2-8 catalyst (1.6 mol%, 20 mg), nitrile (0.25 mmol), internal standard (*n*-hexadecane, 25 µL), solvent (2 mL) and a 25% aqueous solution of NH_3 (200 µL) in that order. The vial was placed into a 300 mL Parr steel autoclave equipped with a drilled aluminum plate that accommodates up to 7 uniform reaction glasses (8 mL). The autoclave was then flushed with hydrogen twice at 30 bar, pressurized with hydrogen and placed into an aluminum block which was heated to the required temperature. On completion of the reaction the autoclave was put into a water bath to accelerate cooling to r. t. After releasing non-consumed H_2 gas, the vials were removed from the autoclave whereupon the catalyst was separated by centrifugation. A sample of the clear supernatant was collected, diluted with ethyl acetate and analyzed by GC (all GC-yields are average values from at least 2 runs; the calibration curve of the starting materials as well as the products were obtained using the commercially available materials).

Isolation of amines **2** *as the corresponding HCl salts* **5** (**Table 4**). The supernatant obtained after separating the catalyst by centrifugation was evaporated to dryness under reduced pressure. The residue was dissolved in AcOEt (2 mL), cooled in an ice bath and treated with a 1.25 M solution of HCl in methanol (0.2-0.3 mL). The formed precipitate was filtered, washed with *n*-hexane (2 x 0.5 mL) and dried *in vacuo.*

3. Results and discussion

3.1. Catalyst characterization

The characterization of the active catalyst B_{12}@CeO_2-8 by scanning transmission electron microscopy (STEM) disclosed two different Co phases in the material (**Fig. 1**). One of them consists of Co-oxide

View Article Online
DOI: 10.1039/C7CY01577A

particles with a large size variation, whereas the other is relatively finely dispersed. Notably, due to the low contrast of these species it was not possible to directly image the Co phase with the electron detectors. Hence, EDX elemental maps were acquired to locate the Co species (**Fig. 1** C).

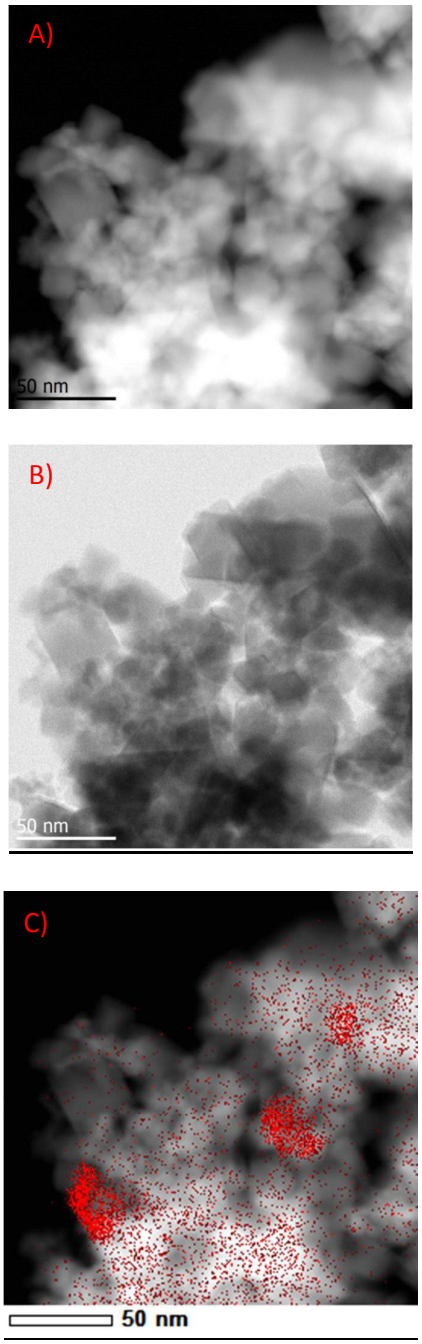

Fig. 1. A) HAADF-STEM image and B) ABF-STEM image of fresh B_{12}@CeO_2-8 demonstrating the general morphology of the support. For contrast reasons, Co containing phases cannot be identified directly. C) Overlay of Co-EDX-elemental map and corresponding HAADF map showing the distribution of the Co on the support. Note a Co-particle phase with a high concentration of Co-signal and a more disperse phase on the ceria with a lower density of Co-signal.

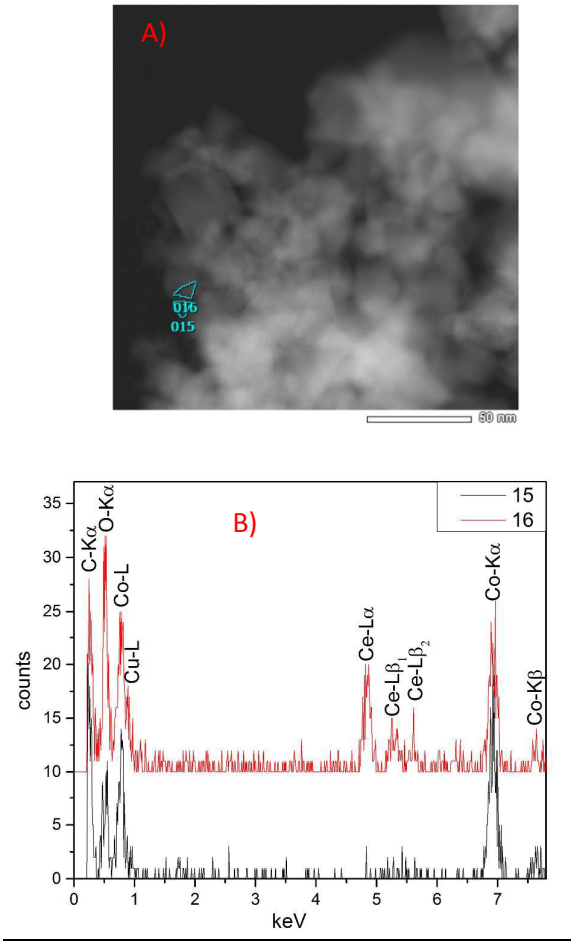

Fig. 2. A) EDX-spectra of the regions marked in the HAADF-image B). Spectrum 15 shows the presence of Co and O in a region where there is no overlap with the ceria support as indicated in spectrum16.

The nature of the particles was determined in cases where a Co-containing particle was located that was partially detached from the ceria support (**Fig. 2**). EDX spectroscopy revealed the presence of oxygen together with the cobalt signal. Hence, we conclude that the particles consist of Co-oxide, potentially Co_3O_4 (Fig TEM S1.)

X-ray diffraction analysis (XRD) and X-ray photoelectron spectroscopy (XPS) were also used to characterize the structure of the catalyst. Unfortunately, the XRD measurements solely revealed the pertinent pattern of pure ceria. The concentration of the Co-containing species was too low or/and this phase was too amorphous. The XPS measurement detected Co species at the active surface, however due to low concentration the noisy spectra

View Article Online
DOI: 10.1039/C7CY01577A

could not evaluated any further (cf. fig. XPS-S1). Similarly, the N 1s spectrum only exhibits one signal at 400 eV that might be assigned to pyrrolic-type N atoms. Again, no further evaluation of the spectrum was possible.

3.2. Nitrile Hydrogenation

The catalytic hydrogenation of benzonitrile **1** to benzylamine **2** (**Scheme 1**, R = Ph) was chosen as the model reaction to evaluate

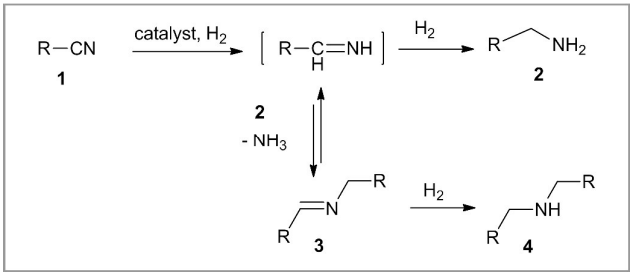

Scheme 1. Hydrogenation of nitriles and proposed mechanism

Table 1. Hydrogenation of benzonitrile: Optimization of reaction conditions.

	pyrolysis T (°C)	H_2 (bar)	T (°C)	NH_3(aq) (mL)	conv (%)[b]	**2**/**3**+**4** molar ratio[b]	GC yield of **2** (%)
1	1000	50	140	-	52	33/67	-
2	900	50	140	-	48	25/75	-
3	800	50	140	-	99	60/40	-
4	700	50	140	-	99	65/35	-
5	1000	50	140	0.1	>99	95/5	90
6	900	50	140	0.1	>99	95/5	90
7	800	50	140	0.1	>99	93/7	89
8	700	50	140	0.1	>99	95/5	87
9	1000	30	120	0.2	0	-	-
10	900	30	120	0.2	>99	97/3	88
11	800	30	120	0.2	>99	>99	94
12	700	30	120	0.2	>99	>99	87
13	800	20	120	0.2	95	>99	83
14	800	30	100	0.2	86	72/28	-
15	800	30	120	0.2	77[c]	70/30	-

[a]*Reaction conditions*: benzonitrile (0.25 mmol), B_{12}@CeO_2 catalyst (1.6 mol %), aqueous NH_3, *i*-PrOH (2 mL), *n*-hexadecane as an internal standard (25 µL), 15 h. [b]Determined by gas chromatography (GC). [c]0.8 mol % of catalyst.

the activity of the produced composites.[20] Initial catalytic tests using 0.25 mmol substrate were conducted in *i*-PrOH at 140 °C and 50 bar H_2 pressure in the presence of 1.6 mol % catalyst loading, (**Table 1**). Catalysts obtained upon pyrolysis at 700 and 800 °C gave rise to full conversion of **1** whereas the higher temperature-treated congeners (900 and 1000 °C) only afforded partial conversion of benzonitrile (**Table 1**, entries 1-4). In all cases the selectivity towards the desired benzylamine was low and *N*-benzylated imine **3** and dibenzylamine **4** were observed as side products in considerable quantities (**Scheme 1**). It is well established that the hydrogenation of nitriles proceeds through an elusive primary imine intermediate that reacts with the just-formed primary amine to furnish a relatively stable secondary imine under concomitant expulsion of ammonia. Catalytic hydrogenation of this secondary imine intermediate then eventually produces the secondary amine as the other side product. Hence, on carrying out the hydrogenation reaction in the presence of aqueous ammonia solution, the formation of the unwanted *N*-benzylated imine **3** was effectively suppressed and accordingly the selectivity towards benzylamine **2** increased dramatically to ~90% for the entire catalyst array (**Table 1**, entries 5-8).

Because of full conversion at 140°C, the reaction temperature and H_2 pressure were reduced in order to examine the performance of the active CeO_2 supported catalysts under milder reaction conditions. Concerning the catalytic transformation conducted in *i*-PrOH at 120 °C and 30 bar H_2 pressure and in the presence of 0.2 mL of aqueous ammonia solution (25 %) the impregnated samples pyrolysed between 700 °C and 900 °C enabled complete substrate conversions and high selectivities towards benzylamine. These results stand in contrast to the performance of the composite material obtained upon pyrolysis at 1000 °C. In this particular case, we could not observe any catalytic activity at all (**Table 1**, entries 9-12). As depicted in **Fig. 3** the time-concentration profile for the given transformation further demonstrates the pronounced difference in catalyst activity for samples pyrolysed at different temperatures. Interestingly, thermal treatment at 800 °C afforded the most active composite material and thus we used this sample as standard catalyst B_{12}@CeO_2-8. It is noteworthy, further reduction of reaction temperature and H_2 pressure as well as reducing the catalyst loading did not improve the outcome of the given transformation. Actually, lowering the temperature and catalyst

View Article Online
DOI: 10.1039/C7CY01577A

amount resulted in a drastic decrease of the selectivity towards the desired primary amine (**Table 1**, entries 13-15).

We anticipated that the pyrolysis step is indispensable for the impregnated material to develop catalytic activity. Indeed, no substrate conversion was observed when the reaction was carried out in the presence of pristine vitamin B_{12} or merely impregnated CeO_2 (**Table 2**, entries 2 and 3). It is known, non-supported vitamin $B_{12,}$ which was decomposed at 800 °C under inert conditions prior to use, exhibited moderate activity for the generation of benzylamine from benzonitrile (**Table 2**, entry 4), whereas annealed ceria itself does not show any catalytic activity (**Table 2**, entry 5). To our surprise, the ability of thermally treated cyanocobalamin to activate molecular hydrogen for nitrile reduction completely vanished upon separate addition of annealed ceria to the reaction mixture (**Table 2**, entry 6).

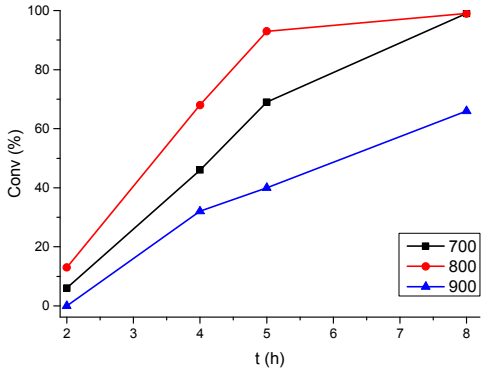

Fig. 3. Time-concentration profile for the heterogeneous hydrogenation of benzonitrile (0.25 mmol) catalysed by B_{12}@CeO_2-7, -8 and -9, respectively) (1.6 mol%) H_2 (30 bar), aqueous NH_3 (0.2 mL), *i*-PrOH (2 mL), *n*-hexadecane as internal standard (25 µL), 120 °C.

Table 2. Hydrogenation of benzonitrile: Catalyst variation.[a]

	Catalyst	Pyrolysis T (°C)	Conv (%)[b]	**2** (%)[b]
1	B_{12}@CeO_2-8	800	>99	94
2	B_{12}@CeO_2	No pyrolysis	0	-
3	Vit B_{12}	No pyrolysis	0	-
4	Vit B_{12}	800	42	23
5	CeO_2[c]	800	0	-
6	B_{12}-8 + CeO_2-8	800	0	-

[a]*Reaction conditions*: benzonitrile (0.25 mmol), catalyst (1.6 mol%), H_2 (30 bar), aqueous NH_3 (0.2 mL), *i*-PrOH (2 mL), *n*-hexadecane as internal standard (25 µL), 120 °C, 15 h. [b]Determined by gas chromatography (GC). [c]20 mg of CeO_2 were used.

We further investigated the influence of the solvent on the outcome of the benchmark reaction. The use of ethanol resulted in a slightly decreased selectivity compared to *i*-PrOH (**Table 3**, entries 1 and 2) whereas less polar aprotic solvents such as THF provided excellent results in terms of yield and selectivity (**Table 3**, entry 3). In contrast, the similar structured di-*n*-butylether turned out to be less selective (**Table 3**, entry 4). Moreover, full conversion was retained when the hydrogenation reaction was conducted in toluene or *n*-heptane but a severe decline of benzylamine selectivity was observed for these aprotic and apolar reaction media (**Table 3**, entries 4 and 5). Apparently, here the equilibrium between **2** and **3** is retarded due to the lower polarity in these solvents. In all cases the addition of aqueous ammonia solution proved to be crucial for obtaining decent substrate conversion.

With optimized reaction conditions in hand (**Table 1**, entry 11) we then elaborated the substrate scope and the corresponding results are summarized in **Table 4**.

Table 3. Hydrogenation of benzonitrile: Variation of the solvent.[a]

	Solvent	Conv (%)[b, c]	**2**/**3**+**4**[b]	**2** (%)[b]
1	*i*-PrOH	>99 (33)	>99	94
2	EtOH	>99 (19)	90/10	87
3	THF	>99 (29)	>99	98
4	dibutyl-*n*-ether	>99(0)	90/10	76
5	toluene	>99 (20)	90/10	85
6	*n*-heptane	>99 (6)	80/20	63

[a]Reaction conditions: benzonitrile (0.25 mmol), B_{12}@CeO_2-8 (1.6 mol%), H_2 (30 bar), aqueous NH_3 (0.2 mL), solvent (2 mL), *n*-hexadecane as an internal standard (25 µL), 120 °C. [b]Determined by GC. [c]Numbers in parentheses refer to conversions (%) in the absence of aqueous NH_3 solution.

A variety of electron-rich and -deficient aryl nitriles displayed good reactivity in the given transformation and the formed primary amines were readily isolated as HCl salts in yields up to 92 % (**Table 4**, entries 2-9). Note here that the catalytic system is well tolerant of sensitive chloro derivatives (**Table 4**, entries 7 and 8). Yet, *p*-bromobenzonitrile is prone to hydrodehalogenation and only poor conversion (60%) was observed when the hydrogenation experiment was performed in the presence of 0.2 mL NH_3 solution. Rewardingly, on doubling the amount of base additive the reaction was brought to completion and afforded a 75/25 mixture composed of *p*-bromobenzylamine and untagged amine (**Table 4**, entry 10). Apparently, steric congestion as in the case of *ortho*-substituted aryl nitriles does not hamper the reaction process. Transposing chloro as well as methoxy groups from *para* to the more demanding *ortho* position gave rise to only a slight decrease of the selectivity towards the desired substituted benzylamine (**Table 4**, entries 3, 4 and 7, 8). Next, the substrate scope was extended to more challenging heterocyclic nitriles. Among these, 3- and 4-cyanopyridine were selectively hydrogenated to afford the desired aminomethyl-tethered pyridine under optimized conditions (**Table 4**, entries 11 and 12). However, the B_{12}@CeO_2-8 standard catalyst did not exhibit any activity for the heterogeneous hydrogenation of 2-cyanopyridine. Even at elevated temperature and pressure (140 °C, 50 bar) as well as on doubling the catalyst loading (3.2 mol%) it was not possible to convert this substrate. Apparently, the spatial proximity of the pyridine nitrogen atom and the 2-cyano group gives rise to a coordination sphere that effectively blocks catalytically active cobalt centers in the composite material. Accordingly, on choosing 2-cyanofurane as substrate which incorporates an oxygen donor atom with a lower propensity to

View Article Online
DOI: 10.1039/C7CY01577A

coordinate, the reaction was successful and the corresponding furfuryl amine was isolated in 39% yield (**Table 4**, entry 13).
Moreover, other substrates including alicyclic, aliphatic as well as benzylic nitriles gave the corresponding primary amines with excellent selectivity upon reaction with H_2 gas (**Table 4**, entries 14-18). The isolated phenethylamine products represent strategic building blocks in the synthesis of biologically active molecules.

Table 4. Catalytic hydrogenation of various nitriles: Scope and limitations.[a]

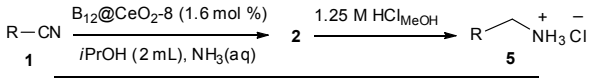

	nitrile	conv (%)[b]	**2** (%)[c]	**5** (%)[d]
1	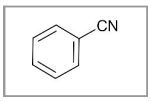	>99[e]	96	87
2	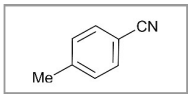	>99	91	86
3	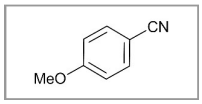	>99	92	85
4	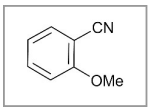	>99	88	85
5	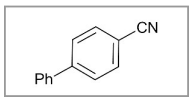	>99	99	92
6	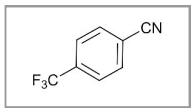	>99	91	86
7	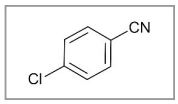	>99[f]	96	88
8	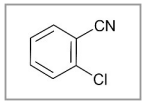	>99	86	82
9	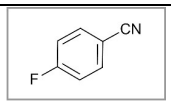	>99	84	78
10	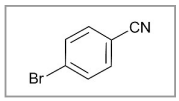	>99[g]	67	-
11	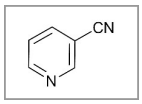	>99[f]	90	85[h]
12	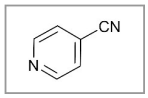	>99[f]	95	89[h]
13	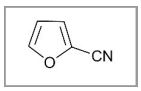	>99[f]	74[i]	39
14	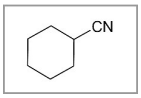	>99	99	97
15	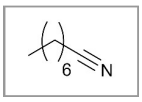	>99	93	90
16	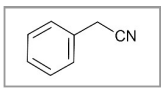	>99	93	90
17	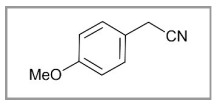	>99	88	88
18	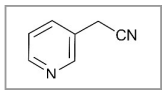	>99[f,l]	98	92

[a]*Reaction conditions*: **1** (0.25 mmol), catalyst (1.6 mol%), H_2 (30 bar), aqueous NH_3 (0.2 mL), *i*-PrOH (2 mL), *n*-hexadecane as internal standard (25 µL), 120 °C, 15 h. [b] Determined by gas chromatography (GC). [c]GC yield. [d]Isolated yield. [e]8 h. [f]3.2 mol% of catalyst. [g] 0.4 mL of aqueous NH_3. [h]Product isolated as the pure amine. [i]The reaction crude contains 80% of **2** and 10% of 2-furoic acid (^{1}H NMR analysis). [l]At 50 bar H_2.

The potential of the B_{12}@CeO_2-8 composite to function as heterogeneous hydrogenation catalyst was further examined with other reducible substrates (**Scheme 2**). To our delight, nitrobenzene **6** was smoothly converted into aniline upon reaction at 120 °C and 30 bar both in THF and *i*-PrOH. In addition, benzaldehyde **8** and acetophenone **9** provided the desired alcohols **10** and **11** at 140 °C and 50 bar. In these cases, the best results with respect to selectivity (99 and 95 %, respectively) were achieved in THF as

View Article Online
DOI: 10.1039/C7CY01577A

reaction medium. Only a slight amount of ethylbenzene (5 %) resulting from catalytic deoxygenation of **10** was found when the hydrogenation reaction was conducted with acetophenone as substrate. Finally, carbonyl derivatives **7** and **8** underwent reductive amination in the presence of aqueous ammonia solution whilst using *i*-PrOH as solvent.

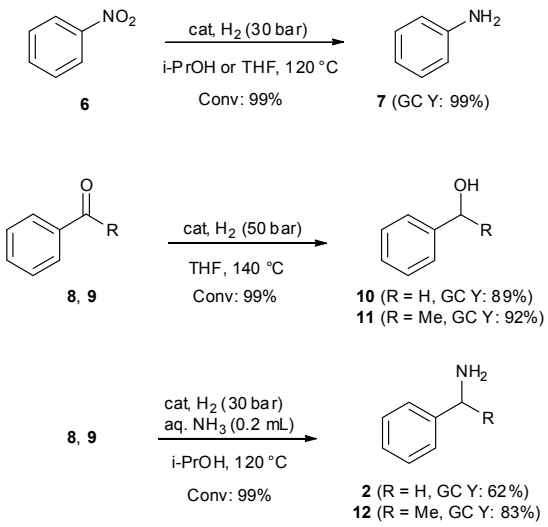

Scheme 2. *Reaction conditions*: substrate (0.25 mmol), B_{12}@CeO_2-8 catalyst (1.6 mol%), H_2 (30-50 bar), *i*-PrOH or THF (2 mL) as solvent, 15 h, conversion and yield were determined by GC analysis using *n*-hexadecane (25 µL) as internal standard.

3.3. Catalyst recycling

For testing the recyclability of B_{12}@CeO_2-8 in the hydrogenation reaction of benzonitrile, five consecutive reactions deploying either 0.25 or 0.5 mmol substrate were conducted with one individual catalyst loading (**Table 3**). After each reaction interval (15 h) the solid matter was separated by centrifugation and reused in the next run. During the first four separation steps the product yield remained constant at a value of ca. 90-94%. In the fifth run a moderate loss of activity was observed.

Table 5. Recycling of B_{12}@CeO_2-8 for the hydrogenation of benzonitrile.[a]

Run	1	2	3	4	5
GC Y (%)	91	91	91	90	83
GC Y (%)[b]	93	93	94	90	84

[a]*Reaction conditions*: benzonitrile (0.25 mmol), B_{12}@CeO_2-8 catalyst (1.6 mol%), H_2 (30 bar), aqueous NH_3 (0.2 mL), *i*-PrOH (2 mL), *n*-hexadecane as an internal standard (25 µL), 120 °C, reaction time 15 h. [b] Benzonitrile (0.5 mmol).

ICP analysis of the supernatant collected after each run revealed that leaching of any soluble cobalt species into the liquid phase was not detectable during the course of the reaction. In order to exclude the emergence of cobalt compounds that function as homogeneous catalysts for the activation of H_2 one reaction batch was interrupted after a period of 2 h which corresponds to a low conversion of benzonitrile (≤ 20%). The solid fraction was then separated by filtration of the hot reaction mixture whereupon the hydrogenation process was resumed with the clear filtrate.[21] Complete catalytic inactivity of the latter was observed and from this experimental finding we have to infer that the hydrogenation process facilitated by B_{12}@CeO_2-8 exclusively proceeds in a heterogeneous manner (Fig. S1).

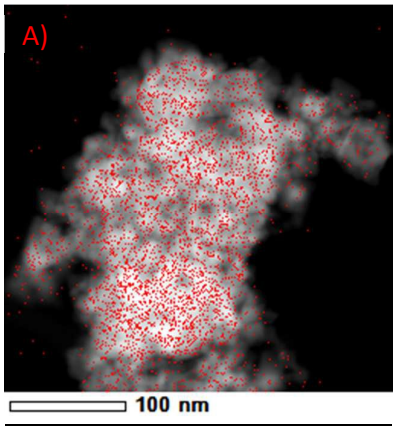

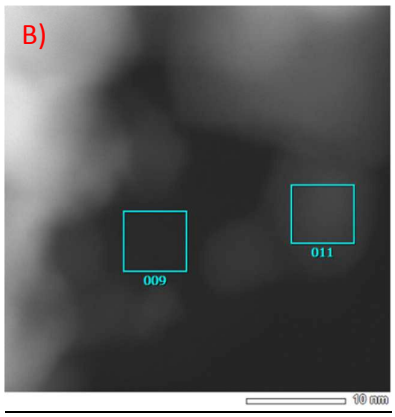

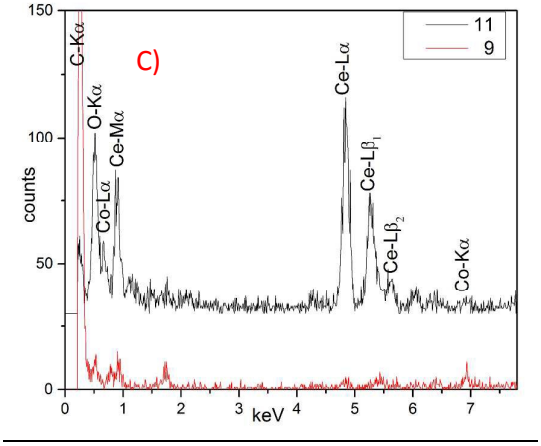

View Article Online
DOI: 10.1039/C7CY01577A

Fig. 4. A) HAADF-STEM image of recycled catalyst overlayed with EDX Co-elemental map showing a disperse distribution of Co. B) HAADF-image of a higher magnified region of A), from where the EDX-spectra C) are taken. The spectrum from region 9 shows a small Co peak where in region 11 with less carbon no Co signal can be identified.

After 5 recycling runs specimen B_{12}@CeO_2-8 was also investigated by STEM. Here, only a distributed Co-phase remains, the particles of the fresh specimen have disappeared as displayed in the corresponding Co-map (Fig. **4** A). However, a carbon phase containing Co attached to the ceria support was found (Fig **4** B and C, also compare Fig. TEM S2 and S3).

4. Conclusion

The synthesis of vitamin B12-derived heterogeneous catalysts active in various hydrogenations is described. Immobilization of natural cyanocobalamin by wet impregnation on ceria and subsequent pyrolysis under inert conditions leads to novel composite material with a carbonaceous cobalt phase and cobalt oxide nanoparticles. The most active catalyst shows good performance in the industrially relevant heterogeneous hydrogenation of nitriles to the corresponding primary amines. Moreover, the catalyst is active for hydrogenation of nitrobenzene, acetophenone, and benzaldehyde.

Acknowledgements

We thank Dr. Matthias Schneider (XRD), Dr. Jörg Radnik (XPS), Mrs Astrid Lehmann (EA) and Mrs Anja Simmula (ICP) for excellent analytic support. R. F. thanks Consiglio Nazionale delle Ricerche (Short Term Mobility Program 2015) for supporting the visit at LIKAT. D. B. thanks EC 7th Framework Program (Project REGPOT-CT-2013-316149-InnovaBalt) for supporting the research stay at LIKAT.

Notes and references

[1] (a) A. Schaetz, M. Zeltner, W. J. Stark, *ACS Catal.* 2012, **2**, 1267; (b) B. F. Machado, P. Serp, *Catal. Sci. Technol.* 2012, **2**, 54; (c) J. Albero, H. Garcia, *J. Mol. Catal. A: Chem.* 2015, **408**, 296.

[2] (a) R. Zhou, M. Jaroniec, S.-Z. Qiao, *ChemCatChem* 2015, **7**, 3808-3817; (b) C. N. R. Rao, K. Gopalakrishnan, A. Govindaraj, *Nano Today* 2014, **9**, 324.

[3] (a) X. Fan, G. Zhang, F. Zhang, *Chem. Soc. Rev.* 2015, **44**, 3023; (b) S. R. Stoyanov, A. V. Titov, P. Král, *Coord. Chem. Rev.* 2009, **253**, 2852; (c) H. Liu, Y. Liu, D. Zhu, *J. Mater. Chem.* 2011, **21**, 3335.

[4] (a) S. Sahin, P. Mäki-Arvela, J.-P. Tessonnier, A. Villa, S. Reiche, S. Wrabetz, D. Su, R. Schlögl, T. Salmi, D. Y. Murzin, *Applied Catalysis A: General* 2011, **408**, 137; (b) P. Chen, L. Chew, M. Kostka, A. Muhler, M. Xia, W. *Catal. Sci. Technol.* 2013, **3**, 1964; (c) P. Chen, F. Yang, A. Kostka, W. Xia, *ACS Catal.* 2014, **4**, 1478; (d) J. Long, Y. Zhou, Y. Li, *Chem. Commun.* 2015, **51**, 2331; (e) Z. Wei, J. Wang, S. Mao, D. Su, H. Jin, Y. Wang, F. Xu, H. Li, Y. Wang, *ACS Catal.* 2015, **5**, 4783; (f) Z. Li, J. Li, J. Liu, Z. Zhao, C. Xia, F. Li, *ChemCatChem* 2014, **6**, 1333; (g) Y. Marco, L. Roldán, S. Armenise, E. García-Bordejé, *ChemCatChem* 2013, **5**, 3829; (h) S. Pisiewicz, D. Formenti, A.-E. Surkus, M.-M. Pohl, J. Radnik, K. Junge, C. Topf, S. Bachmann, M. Scalone, M. Beller, *ChemCatChem 2016,* **8**, 129-134; (i) R. V. Jagadeesh, A. Surkus, H. Junge, M. Pohl, J. Radnik, J. Rabeah, H. Huan, V. Schünemann, A. Brückner and M. Beller, *Science*, 2013, **342**, 1073–1076.

[5] (a) Chan-Thaw, C. E. Villa, A. Katekomol, P. Su, D. Thomas, A. Prati, L. *Nano Lett.* 2010, **10**, 537; (b) X. Ning, H. Yu, F. Peng, H. Wang, *J. Catal.* 2015, **325**, 136; (c) J. Deng, H.-J. Song, M.-S. Cui, Y.-P. Du, Y. Fu, *ChemSusChem* 2014, **7**, 3334; (d) Y. Chen, L. Fu, Z. Liu, *Chem. Commun.* 2015; (e) Y. Chen, S. Zhao, Z. Liu, *PCCP* 2015, **17**, 14012; (f) A. V. Iosub, S. S. Stahl, *Org. Lett.* 2015 (f) X. Cui, Y. Li, S. Bachmann, M. Scalone, A.-E. Surkus, K. Junge, C. Topf, M. Beller, *J. Am. Chem. Soc. 2015,* **137**, 10652.

[6] L. Zhang, A. Wang, W. Wang, Y. Huang, X. Liu, S. Miao, J. Liu, T. Zhang, *ACS Catal.* 2015, 6563.

[7] (a) Q. Lai, Q. Gao, Q. Su, Y. Liang, Y. Wang, Z. Yang, *Nanoscale* 2015, **7**, 14707; (b) F. Jaouen, S. Marcotte, J.-P. Dodelet, G. Lindbergh, *J. Phys. Chem. B* 2003, **107**, 1376; (c) J. Han, Y. J. Sa, Y. Shim, M. Choi, N. Park, S. H. Joo, S. Park, *Angew. Chem. Int. Ed.* 2015, **54**, 12622; (d) Y. Su, Y. Zhu, H. Jiang, J. Shen, X. Yang, W. Zou, J. Chen, C. Li, *Nanoscale* 2014, **6**, 15080; (e) A. A. Gewirth, M. S. Thorum, *Inorg. Chem.,* 2010, **49**, 3557.

[8] C. H. Choi, C. Baldizzone, J.-P. Grote, A. K. Schuppert, F. Jaouen, K. J. J. Mayrhofer, *Angew. Chem. Int. Ed.* 2015, **54**, 12753.

[9] (a) D. Chauhan, P. Kumar, C. Joshi, N. Labhsetwar, S. K. Ganguly, S. L. Jain, *New J. Chem.* 2015, **39**, 6193; (b) J. Xi, Y. Xia, Y. Xu, J. Xiao, S. Wang, *Chem. Commun.* 2015, **51**, 10479.

[10] (a) F. A. Westerhaus, R. V. Jagadeesh, G. Wienhöfer, M. Pohl, J. Radnik, A. Surkus, J. Rabeah, K. Junge, H. Junge, M. Nielsen, A. Brückner and M. Beller, *Nat. Chem.*, 2013, **5**, 537; (b) R. V. Jagadeesh, H. Junge, M.-M. Pohl, J. Radnik, A. Brückner, M. Beller, *J. Am. Chem. Soc.* 2013, **135**, 10776; (c) R. V. Jagadeesh, H. Junge, M. Beller, *Nat Commun* 2014, **5** ; (d) T. Stemmler, F. A. Westerhaus, A.-E. Surkus, M.-M. Pohl, K. Junge, M. Beller, *Green Chem.* 2014, **16**, 4535; (e) R. V. Jagadeesh, D. Banerjee, P. B. Arockiam, H. Junge, K. Junge, M.-M. Pohl, J. Radnik, A. Brückner, M. Beller, *Green Chem.* 2015, **17**, 898; (f) R. V. Jagadeesh, T. Stemmler, A.-E. Surkus, M. Bauer, M.-M. Pohl, J. Radnik, K. Junge, H. Junge, A. Brückner, M. Beller, *Nat. Protocols* 2015, **10**, 916; (g) S. Pisiewicz, T. Stemmler, A.-E. Surkus, K. Junge, M. Beller, *ChemCatChem* 2015, **7**, 62; (h) F. A. Westerhaus, I. Sorribes, G. Wienhöfer, K. Junge, M. Beller, *Synlett* 2015, **26**, 313.

[11] D. Formenti, F. Ferretti, C. Topf, A.-E. Surkus, M.-M. Pohl, J. Radnik, M. Schneider, K. Junge, M. Beller, F. Ragaini, *J. Catal.*, 2017, **351**, 79.

[12] F. Chen, A.-E. Surkus, L. He, M.-M. Pohl, J. Radnik, C. Topf, K. Junge, M. Beller, *J. Am. Chem. Soc.* 2015, **137**, 11718.

[13] M. Giedyk, K. Goliszewska, D. Gryko *Chem. Soc. Rev.,* 2015, **44**, 3391.

[14] S.-T. Chang, C.-H. Wang, H.-Y. Du, H.-C. Hsu, C.-M. Kang, C.-C. Chen, J. C. S. Wu, S.-C. Yen, W.-F. Huang, L.-C. Chen, M. C. Lin, K.-H. Chen, *Energy Environ. Sci.*, 2012, **5**, 5305.

[15] (a) H.-W. Liang, S. Brüller, R. Dong, J. Zhang, X. Feng, K. Müllen, *Nat. Commun.*, 2015, **6**, 7992; (b) M. Dou, D. He, W. Shao, D. Liu, F. Wang, L. Dai, *Chem. Eur. J.* 2016, **22**, 2846.

[16] B. Chen, S. Shang, L. Wang, Y. Zhang, S. Gao, *Chem. Commun.*, 2016, **52**, 481.

[17] (a) A. Trovarelli, *Catal. Rev.: Sci. Eng.*, 1996, 38, 439–520. (b) A. Trovarelli, *Catalysis by ceria and related materials*; Imperial College Press: London, 2002.

View Article Online
DOI: 10.1039/C7CY01577A

[18] (a) R. S. Downing, P. J. Kunkeler, H. van Bekkuum, *Catal. Today*, 1997, **37**, 121; (b) S. Werkmeister, J. Neumann, K. Junge, M. Beller, *Chem. Eur. J.* 2015, **21**, 12226; (c) D. S. Mérel, M. L. T. Do, S. Gaillard, P. Dupau, J.-L. Renaud, *Coord. Chem. Rev.* 2015, **288**, 50; (d) D. B. Bagal, B. M. Bhanage, *Adv. Synth. Catal*. 2015, **357**, 883; (e) S. Werkmeister, K. Junge, M. Beller, *Org. Process Res. Dev*. 2014, **18**, 289; (f) M. Vilches-Herrera, S. Werkmeister, K. Junge, A. Börner, M. Beller, Catal. Sci. Technol., 2014, **4**, 62.
[19] T. Stemmler, F. Chen, S. Pisiewicz, A.-E. Surkus, M.-M. Pohl, C. Topf, M. Beller, *J. Mater. Chem. A*, 2015, **3**, 17728.
[20] For recent examples of Co-catalyzed nitrile hydrogenation see: (a) P. Ji, K. Manna, Z. Lin, X. Feng, A. Urban, Y. Song, W. Lin, *J. Am. Chem. Soc*., 2017, **139**, 7004; (b) J. Long, K. Shen, Y. Li *ACS Catal*., 2017, **7**, 275; (c) R. Adam, C. B. Bheeter, J. R. Cabrero-Antonino, K. Junge, R. Jackstell, M. Beller, *ChemSusChem* 2017, **10**, 842; (d) Z. Shao, S. Fu, M. Wei, S. Zhou, Q. Liu, *Angew. Chem. Int. Ed.* 2016, **55**, 14653; (e) F. Chen, C. Topf, J. Radnik, C. Kreyenschulte, H. Lund, M. Schneider, A.-E. Surkus, L. He, K. Junge, M. Beller, *J. Am. Chem. Soc*., 2016, **138**, 8781; (f) A. Mukherjee, D. Srimani, S. Chakraborty, Y. Ben-David, D. Milstein, *J. Am. Chem. Soc*., 2015, **137**, 8888; (g) P. Schärringer, T. E. Müller, J. A. Lercher, *J. Catal*., 2008, **253**, 167.
[21] J. E. Hamlin, K. Hirai, A. Millan, P. M. Maitlis, *J. Mol. Catal.* 1980, **7**, 543.